

PROCEEDINGS OF THE CONFERENCE “SILICON-2014”, IRKUTSK, JULY 7–12, 2014
SURFACES, INTERFACES,
AND THIN FILMS

Recombination Activity of Interfaces in Multicrystalline Silicon

S. M. Peshcherova^{a*}, E. B. Yakimov^b, A. I. Nepomnyashchikh^a, L. A. Pavlova^a, and O. V. Feklisova^b

^a Vinogradov Institute of Geochemistry, Siberian Branch, Russian Academy of Sciences, Irkutsk, 664033 Russia

^b Institute of Microelectronics Technology and High-Purity Materials, Russian Academy of Sciences, Chernogolovka, Moscow oblast, 142432 Russia

*e-mail: speshcherova@mail.ru

Submitted October 27, 2014; accepted for publication November 5, 2014

Abstract—The electrical activity of grain boundaries in multicrystalline silicon grown from metallurgical silicon by the Bridgman method is investigated by the method of electron-beam induced current. The main tendencies of atypical manifestation of the local electrical activity of $\Sigma 3\{111\}$ and $\Sigma 9\{110\}$ special boundaries are revealed. The structural features of the grain boundaries after selective etching and the impurity-distribution characteristics in multicrystalline silicon are determined by the methods of electron backscattering diffraction and electron-probe microanalysis.

DOI: 10.1134/S1063782615060196

1. INTRODUCTION

Investigation of the electrical activity of grain boundaries in multicrystalline silicon (mc-Si) widely used as a material for photoelectric converters is the most important stage of determining its quality. Despite the impressive amount of publications devoted to studying the electrical and structural properties of interfaces in multicrystalline silicon suitable for the fabrication of both electronic devices and solar cells, many problems still remain unsolved. The results of investigations of the electrical activity of boundaries by the method of electron-beam-induced current (EBIC) showed that they are not always efficient recombination centers [1]. It was established using measurements of the contrast at the grain boundaries (GBs) of solar-quality multicrystalline silicon in the temperature range of 50–300 K that boundaries of a random type (*R*) manifest high electrical activity (the EBIC contrast values reach 40% at 50 K and 15% at 300 K), while the greatest contrast at special boundaries (CLS) does not generally exceed 10% at 50 K and 5% at 300 K [2]. In this case, the local contrast enhancement for such special boundaries as $\Sigma 3\{111\}$ and $\Sigma 9\{110\}$ were attributed to the fact that these boundaries were in the immediate vicinity of incoherent $\Sigma 3\{112\}$ boundaries instead of the effect of impurities [3]. However, the authors of more recent publication [4] explain the sharp contrast enhancement (on average from 10 to 20%) on the grain boundaries in multicrystalline silicon before and after annealing in nickel vapors by the intense precipitation of nickel at the grain boundaries. In this publication, we present the results of investigations of the structural features and the electrical activity of grain boundaries in multicrys-

talline silicon grown from refined metallurgical silicon by the methods of X-ray spectral electron-probe microanalysis (EPMA), electron backscattering diffraction (EBSD), and the electron-beam induced current (EBIC) in the scanning electron microscope. The main purpose of the performed investigations is establishment of the qualitative relation between abnormally large values of contrast at 300 K at the grain boundaries of special and random types, the features of the structure of these boundaries, and the impurity and defect distributions in the bulk of multicrystalline silicon upon its crystallization by the Bridgman method.

2. MATERIALS AND METHODS OF INVESTIGATIONS

We investigated the samples obtained of a transverse cut from the upper portion of a mc-Si ingot grown by the Bridgman method from refined metallurgical silicon with an electrical resistivity of 3.5 Ω cm and an average lifetime of nonequilibrium charge carriers of 4.2 μ s. The content of impurity elements in the mc-Si ingot was determined by the method of inductively coupled plasma mass-spectrometry (ICP-MS, Element 2 Finnegan MAT). The average values of the concentration of elements calculated for several samples along the entire length of the mc-Si ingot are listed in Table 1.

The surface of the sample under investigation was polished mechanically with diamond pastes and chemically in a mixture of HF and HNO₃ acids; then, Al was deposited for the formation of Schottky barriers. The distribution of the recombination rate by the

Table 1. Average values of the impurity concentration in a multicrystalline-silicon ingot, ppm

Element	B	Al	P	Ca	Ti	V	Cr	Mn	Fe	Ni	Cu
Concentration	0.24	0.72	0.09	1.91	0.09	0.003	0.05	0.04	1.22	0.01	0.04

method of electron-induced current was investigated at room temperature using a JEOL JSM 840 scanning electron microscope at a beam energy of 35 keV. We used a beam current of 10^{-10} A, which produces a total intensity of the generation of electron-hole pairs of $5.5 \times 10^{11} \text{ s}^{-1}$. A Keithley 428 current amplifier was used for detection of the signal in the EBIC measurements. The contrast of the EBIC images was measured using the Grayscale function in the Adobe Photoshop CS 5.1 multi software [5, 6].

After chemical surface-layer removal and mechanical polishing of the surface by diamond pastes, the surface of the sample was investigated by the method of X-ray spectral electron-probe microanalysis (JXA8200/JEOL). The types of grain boundaries and the misorientation parameters were determined by the method of backscattering electron diffraction (JIB-Z4500/JEOL).

3. RESULTS AND DISCUSSION

In Fig. 1a, we show the map of grain boundaries of the mc-Si sample under investigation obtained in the EBSD mode. The structural parameters of the grain boundaries for this fragment (1–39) and the contrast value of these grain boundaries calculated from Fig. 1b are listed in Table 2. However, the contrast of many boundaries observed in the backscattering electron mode (Fig. 1c) does not exceed the limit of detection of the method ($\sim 0.5\%$), which can be seen from Table 2. Moreover, the value of the contrast for a number of boundaries is nonuniform along the boundary; therefore, we listed in Table 2 the smallest and largest values of the contrast measured along each boundary. Thus, all the observed boundaries can be divided into three categories:

(i) grain boundaries with variable (nonuniform) contrast; these are the special boundaries $\Sigma 3\{111\}$ (nos. 3, 11, 12, 23, 33, 34), $\Sigma 9\{110\}$ (nos. 5, 24, 35), and $\Sigma 27a\{110\}$ (no. 8);

(ii) grain boundaries exhibiting weak contrast; these are mainly the boundaries $\Sigma 3\{111\}$ (nos. 7, 13, 22, 25, 26, 29, 31, 36, 37) and $\Sigma 9\{110\}$ (no. 21);

(iii) boundaries with uniform pronounced contrast; these are boundaries with random orientation R : (nos. 9, 14–20, 27–32, 38, 39), boundaries $\Sigma 15\{210\}$ (nos. 6, 10), $\Sigma 27b\{210\}$ (no. 1), and $\Sigma 3\{111\}$ (no. 4) that compose the basic part of the boundaries of this type.

The special boundaries related to the first category were especially interesting. In Fig. 1b, it can be seen that, in the sample under investigation, the contrast of individual portions of special boundaries, which are mainly the joints of their portions or the places of breaks, is quite high. This is consistent with the fact that, alongside the boundaries R , high electrical activity can also be manifested by the CLS boundaries, the characteristic feature of which is a high concentration of microdefects [7]. According to Table 2, the largest values of contrast reach 20% for the special boundaries $\Sigma 3\{111\}$ on some portions and 24% for the boundaries $\Sigma 9\{110\}$; the smallest values of contrast for the major-

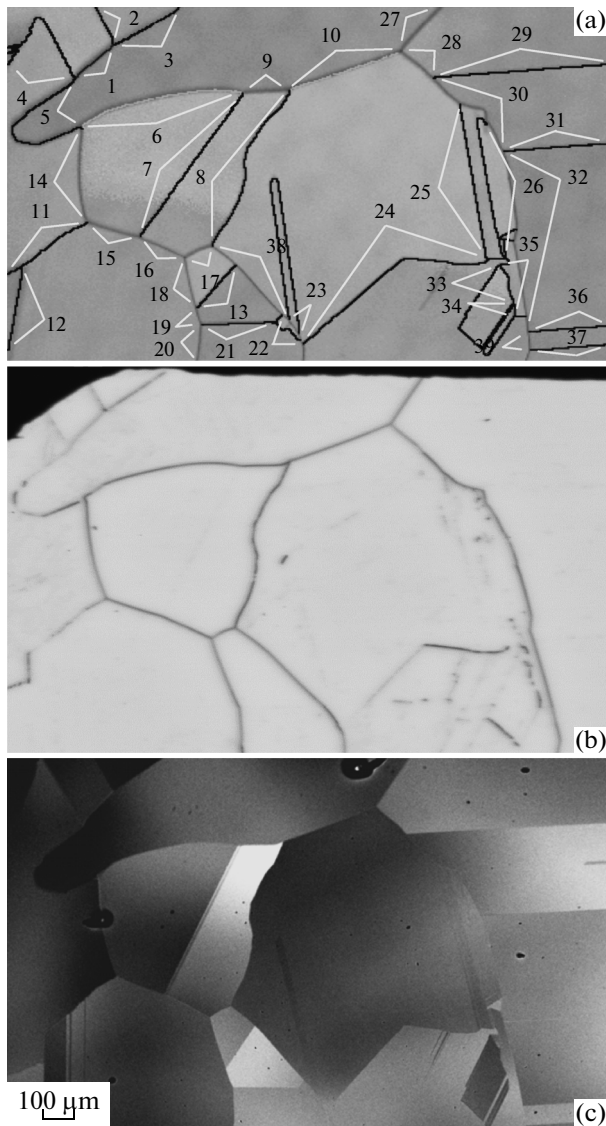


Fig. 1. Images of the mc-Si polished surface obtained in the (a) EBSD, (b) EBIC, and (c) backscattered electrons modes.

Table 2. General characteristics of grain boundaries, GBs (according to the numeration in Fig. 1a)

GB no.	Types of GB	Parameters of the misorientation of neighboring grains		EBIC contrast along GB, %	
		angle, deg	rotation axis	min	max
1	$\Sigma 27b$	35.64	-210	7.2	7.9
2	$\Sigma 9$	38.95	011	7.9	9.3
3	$\Sigma 3$	59.42	1-11	6.5	20.8
4	$\Sigma 3$	59.99	-1-11	4.3	7.9
5	$\Sigma 9$	39.06	0-1-1	2.1	20.8
6	$\Sigma 15$	44.99	0-1-2	12.2	18
7	$\Sigma 3$	59.09	-1-11	0.7	2.8
8	$\Sigma 27a$	31.21	101	9.3	20.1
9	<i>R</i>	29.71	1-2-1	17.3	22.3
10	$\Sigma 15$	50.1	02-1	12.9	15.1
11	$\Sigma 3$	59.98	-1-11	0.7	12.9
12	$\Sigma 3$	59.99	-111	0	18
13	$\Sigma 3$	59.79	1-1-1	0	0.7
14	<i>R</i>	50.29	-4-32	11.5	18.7
15	<i>R</i>	29.7	142	15.1	18
16	<i>R</i>	53.6	110	15.1	16.5
17	<i>R</i>	18.93	2-1-1	11.5	16.5
18	<i>R</i>	49.45	-21-4	10.8	12.2
19	<i>R</i>	33.68	-342	10.8	11.5
20	<i>R</i>	56.65	2-1-2	18	19.4
21	$\Sigma 9$	39.4	0-1-1	0	0.7
22	$\Sigma 3$	59.89	-1-11	0	5
23	$\Sigma 3$	59.8	11-1	0	20.1
24	$\Sigma 9$	39.3	-10-1	0.7	24.5
25	$\Sigma 3$	59.74	-1-11	0	4.3
26	$\Sigma 3$	60	11-1	0	5
27	<i>R</i>	48.63	4-21	11.5	12.9
28	<i>R</i>	47.64	11-2	8.6	11.5
29	$\Sigma 3$	59.98	1-11	0	0.7
30	<i>R</i>	38.86	041	15.1	19.4
31	$\Sigma 3$	59.88	11-1	0	1.4
32	<i>R</i>	47.16	12-1	12.9	16.5
33	$\Sigma 3$	59.99	-1-11	0	18
34	$\Sigma 3$	59.74	-1-11	0	16.5
35	$\Sigma 9$	38.97	0-1-1	3.6	18.7
36	$\Sigma 3$	59.97	1-11	0.7	1.4
37	$\Sigma 3$	59.95	11-1	0	0.7
38	<i>R</i>	52.08	-41-2	11.5	13.7
39	<i>R</i>	23.41	-11-2	10.8	17.3

ity of these boundaries is smaller than 1%. As is known, the special boundaries ($\Sigma 3$, $\Sigma 9$), as a rule, exhibit weak contrast in a wide temperature range

[8–12]. This type of boundaries is considered as the least electrically active due to the features of their structure, and most of them do not exhibit pro-

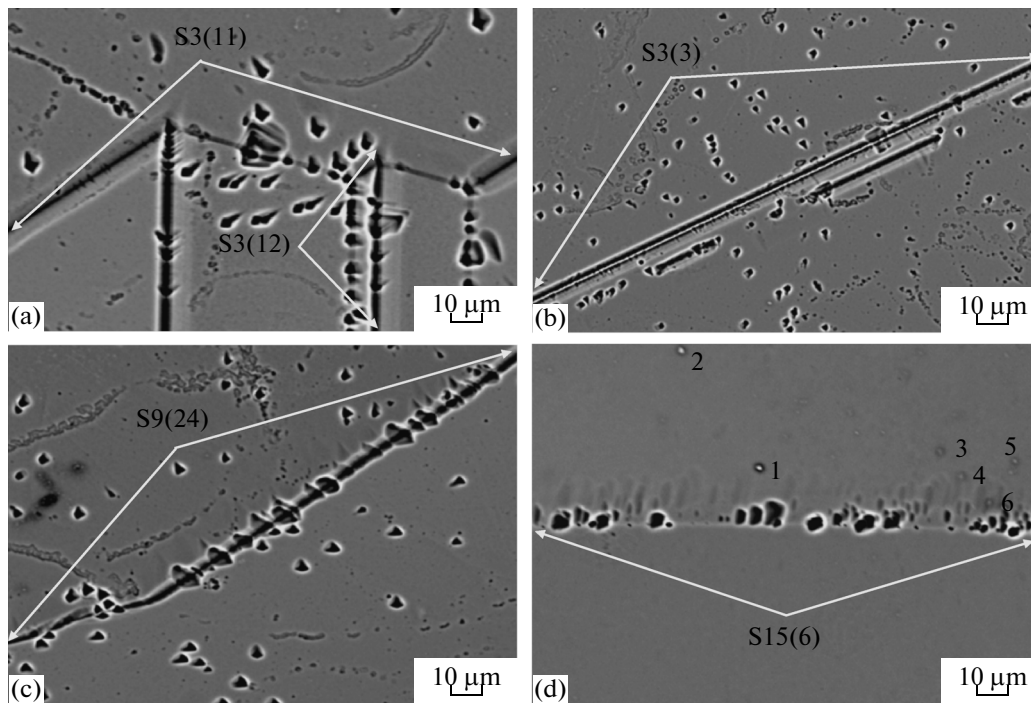


Fig. 2. Images produced via backscattered electrons for various portions of an mc-Si etched surface with the grain boundaries numbered according to Fig. 1a and Table 2: (a) $\Sigma 3$ —boundaries nos. 11 and 12; (b) $\Sigma 3$ —boundary no. 3; (c) $\Sigma 9$ —boundary no. 24; and (d) $\Sigma 15$ —boundary no. 6 and precipitates 1–6 in the grain.

nounced contrast in the EBIC mode at room temperature. Few observations of an increase in contrast near boundaries of this type at room temperature were explained by the segregation of metal impurities (Ni, Fe, Cr, etc.) artificially introduced by diffusion into the samples under investigation [4, 11], with the change in the electrical activity of boundaries depending on the degree of metal contamination.

In the secondary-electron mode, we investigated the sample surface treated preliminary for 10 s with selective etchant HF : HNO₃ : CH₃COOH (in the ratio 5 : 10 : 2 of the volume fractions, respectively). Investigations of the structure of the etched surface enable us to reveal the general tendencies of the structural features of grain boundaries inducing the degree of their recombination activity. For example, special boundaries belonging to the second type represent even straight lines without pronounced violations and visible defects. In contrast to those, special boundaries from the first category are not straight lines in terms of their entire length, and have local breaks, which are clearly seen at large magnifications. For example, the joint of boundaries $\Sigma 3$ no. 11 and no. 12 represents a region of local breakage of boundary no. 11 and boundary no. 12 (conjugated to it) along which the dislocation etchings pits are successively located in the case of the presence of a set of dislocations (Fig. 2a).

It should be noted that the highest contrast is observed exactly in this portion of boundary no. 12. Boundary no. 3 also shows the highest contrast in

regions of the presence of dislocation etching pits located along the boundary line (Fig. 2b). Directly in the region of boundaries $\Sigma 3$, we observed the lowest number of dislocations as evidenced by the solitary etching pits on the boundary lines themselves and their high density near the boundaries. However, the electrically active special boundaries with a lower degree of symmetry ($\Sigma 9$, $\Sigma 15$, $\Sigma 27a$, and $\Sigma 27b$) contain dislocations, the density of which, according to the number of etching pits, appreciably increases in the places of bends and breaks (Figs. 2c and 2d).

Upon investigation by the method of electron-probe microanalysis, it is found that it is possible to observe various precipitates and the features of their arrangement in the mc-Si macrostructure. For example, the accumulation of precipitates was observed in one of the large grains (Fig. 2d). It is worth noting that the arrangement of precipitates (the largest of them are marked in Figs. 2d, 1–6) is really close to special boundary no. 6; however, in the region of the boundary itself, no similar precipitates were revealed. The compositions of precipitates (1–6) are listed in Table 3.

As can be seen from Tables 1 and 3, the main fraction of metal impurities is present in the crystal bulk in the form of precipitates of variable composition. The distribution of impurities in the mc-Si structure occurs predominantly over grain regions; it is most likely that the precipitates occupy energetically favorable positions in microdefects (dislocations, cavities, pores,

Table 3. Compositions of precipitates 1–6 marked in Fig. 2d, wt %

Element	Si	O	C	Fe	Ca	Cr	Al	Cu	Zn
1	62.5	22.8	0	0	14.7	0	0	0	0
2	28.8	6.2	40.5	18.1	0	5.0	1.3	0	0
3	27.9	24.9	35.1	4.9	7.2	0	0	0	0
4	52.9	0	0	39.1	0	8.0	0	0	0
5	7.8	0	6.1	75.8	0	10.1	0	0	0
6	57.4	0	0	0	0.6	0	0	25.8	16.1

etc.). Directly in the grain-boundary region, no precipitates were revealed.

4. CONCLUSIONS

Investigations of the electrical and structural features of grain boundaries of various types in multicrystalline silicon grown by the Bridgman method from refined metallurgical silicon enabled us to determine the principal factors significantly affecting the recombination activity of special grain boundaries. At places of the manifestation of a high degree of electrical activity by the boundaries, which is confirmed by the limiting values of the contrast reaching 20% for the boundaries $\Sigma 3\{111\}$ and 24% for the boundaries $\Sigma 9\{110\}$ at room temperature, the presence of dislocations is revealed. Inside the grains, precipitates, the concentration of which appreciably increased near the boundaries, were observed. The distinction in the behavior of special boundaries in the samples under investigation from those in mc-Si crystals grown by other methods can be caused by the structural features of the boundaries themselves, the amount of impurities present in the initial material (metallurgical silicon), and also the conditions of the segregation of impurities for this method of mc-Si growth.

ACKNOWLEDGMENTS

The principal results of the investigations were obtained with the use of the material–technical depot of the Shared Service Center of the Siberian Branch,

Russian Academy of Sciences, “Baikal Analytical Center”.

REFERENCES

1. J. Chen, T. Sekiguchi, D. Yang, F. Yin, K. Kido, and S. Tsurekawa, *J. Appl. Phys.* **96**, 5490 (2004).
2. S. Tsurekawa, K. Kido, and T. Watanabe, *Mater. Sci. Eng. A* **462**, 61 (2007).
3. J. Chen, T. Sekiguchi, D. Yang, F. Yin, et al., *J. Appl. Phys.* **96**, 5490 (2004).
4. Zh. Xi, D. Yang, J. Chen, and T. Sekiguchi, *Mater. Sci. Semicond. Proc.* **9**, 304 (2006).
5. E. B. Yakimov, *Poverkhnost'*, No. 3, 15 (2003).
6. E. B. Yakimov, *J. Phys.: Condens. Matter.* **14**, 13069 (2002).
7. S. M. Peshcherova, A. I. Nepomnyashchikh, L. A. Pavlova, I. A. Eliseev, and R. V. Presnyakov, *Semiconductors* **48**, 476 (2014).
8. B. Cunningham, H. Strunk, and D. G. Ast, *Appl. Phys. Lett.* **40**, 237 (1982).
9. J. Chen, B. Chen, T. Sekiguchi, M. Fukuzawa, and M. Yamada, *Appl. Phys. Lett.* **93**, 105 (2008).
10. S. Brantov, O. Feklisova, and E. Yakimov, *Phys. Status Solidi C* **8**, 1384 (2011).
11. E. B. Yakimov, O. V. Feklisova, and S. K. Brantov, *Solid State Phenom.* **178–179**, 106 (2011).
12. J. Chen, T. Sekiguchi, and D. Yang, *Phys. Status Solidi C* **4**, 2908 (2007).

Translated by V. Bukhanov

Copyright of Semiconductors is the property of Springer Science & Business Media B.V. and its content may not be copied or emailed to multiple sites or posted to a listserv without the copyright holder's express written permission. However, users may print, download, or email articles for individual use.